Dynamic Adaptation of Instantaneous Nonlinear Bipoles in Wave Digital Networks

Alberto Bernardini and Augusto Sarti
Dipartimento di Elettronica, Informazione e Bioingegneria (DEIB)
Politecnico di Milano, Piazza L. Da Vinci 32, 20133 Milano – Italy
[alberto.bernardini,augusto.sarti]@polimi.it

***Abstract*—Accommodating multiple nonlinearities in a modular fashion and with no use of delay elements is a relevant unsolved problem in the literature on Wave Digital (WD) networks. In this work we present a method for adapting instantaneous NonLinear (NL) bipoles characterized by monotonic increasing curves. The method relies on the fact that the characteristic of a NL bipole can be described by a line, which dynamically varies its slope and its intercept according to the actual operating point. This fact allows us to model a NL bipole as a linear real voltage generator with time-varying parameters. Dynamic adaptation makes possible to accommodate multiple nonlinearities in the same WD network, ensuring the absence of delay-free loops. We will show that diodes can be effectively modeled using the presented approach. As an example of application of our method, we present an implementation of a diode-based audio limiter.**

I. Introduction

Wave Digital Filters (WDFs) [1] are particularly suitable for Virtual Analog (VA) modeling [2] as they can be easily designed as digital port-wise representations of analog reference circuits. The circuit elements are characterized by input/ouput functions and the topological connections between such elements are described by scattering matrices, called adaptors. WDFs possess excellent properties such as stability, pseudopassivity and modularity, [1] which are highly desirable in VA applications. Moreover, WDFs theory allows us to easily insert one Non Linear Element (NLE) [3]–[5] in a WD Structure (WDS). However modeling multiple nonlinearities in the same WD network is not a straightforward task. In fact, if proper adaptation conditions are not imposed, delay free loops arise, resulting in instantaneous signal dependencies, which prevent computability. Some partial solutions to this problem are present in the literature. The simplest practical remedy is adding delay elements [6], [7] for breaking the loops; although this trick may lead to instabilities. A safer possible approach is to condensate all the nonlinearities in a single multi-port NLE, as done in [8]–[10], where some WD implementations of diode networks have been presented. However, this approach may lead to complicated systems of equations to solve, which cannot easily be reduced in explicit form. Another method [11] consists of grouping many NLEs at the root of the WDS and using the K method for jointly computing the corresponding scattering vector. Modularity-preserving approaches exist in the literature [12], and they are based on artificial delays and iterative methods. However, in general, there is not a general method, which makes no use of delay elements and modularly solves many separated nonlinearities in the same WD network.

In this work we propose a technique for the adaptation of generic bipoles characterized by NL monotonic increasing curves and always positive derivative. Our idea is describing one-port NLEs as linear real voltage generators with time-varying parameters. We will show this approach turns out to be effective dealing with low and mid-frequency audio signals, while it needs improvements for dealing with high-frequency signals. However, we believe these results might be a good starting point toward the adaptation of more complex nonlinearities and the fully modular modeling of nonlinear WD networks. Instead of using voltage waves, which are more spread in the literature on WDFs [1], we will use rms-power-normalized waves (shortly *power waves*), which are known to be more appropriate for modeling time-varying structures [13], [14]. In Section II we briefly revise the principal components of WD networks and we provide an explicit power wave mapping for the diode, which never appeared in the literature. In Section III we provide a general method for adapting an instantaneous NL bipole. In Section IV we apply the described method to the Shockley diode model. Section V presents an implementation of an audio limiter as an example of application of our results. Section VI concludes this paper.

II. Power Normalized WD Networks

In the Kirchhoff (K) domain, each port of the reference analog circuit is identified by two variables, namely port voltage V and port current I. Conversely, in the WD domain a port is characterized by an incident wave a, a reflected wave b and a reference port impedance (or simply "port impedance") Z, which is a free parameter. Assuming dealing with real power waves and real positive impedances, according to [15], the K-WD transformation can be written as

$$a = \frac{V + ZI}{2\sqrt{Z}} \qquad b = \frac{V - ZI}{2\sqrt{Z}} \tag{1}$$

and the corresponding inverse map is

$$V = (a + b)\sqrt{Z} \qquad I = (a - b)/\sqrt{Z} \ . \tag{2}$$

In the light of this wave definition (1), (2), in this section we describe the most spread WD linear elements and the corresponding adaptation conditions. Moreover we introduce an explicit wave equation based on the Lambert function which

978-0-9928-6265-7/16/$31.00 ©2016 IEEE

characterizes a diode. Finally we revise the scattering matrices usable for implementing the series and parallel adaptors.

A. Linear Resistor

A linear resistor R is characterized by the equation $V = RI$. According to (2), we can write the wave mapping as

$$b = \frac{R - Z}{R + Z} a \ . \tag{3}$$

Therefore the resistor may be adapted setting $Z = R$, so the reflected wave is simply computed as $b = 0$.

B. Real Voltage and Current Generators

A real voltage generator in the K domain can be described by the equation

$$V = RI + V_g \ , \tag{4}$$

where V_g is the voltage source and R is the associated non-zero series resistance. According to (2), we can write the wave mapping as

$$b = \frac{V_g\sqrt{Z} + (R - Z)a}{R + Z} \ . \tag{5}$$

Therefore the real voltage generator is adapted if we set $Z = R$, so the reflected wave is computed as $b = V_g/(2\sqrt{Z})$.
It is worth noticing that (3) may be considered as a particular case of (5) with $V_g = 0$. Analogously, the K equation

$$I = V/R + I_g \ , \tag{6}$$

describing a real current source with parallel resistance R, can be easily fitted into (4) setting $V_g = -RI_g$.

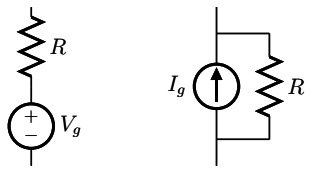

Fig. 1. Real Voltage and Current Generators.

C. Capacitor and Inductor

The power wave mapping of a capacitor, described by the differential equation $I = C\mathrm{d}V/\mathrm{d}t$, where C is the capacitance and $\mathrm{d}/\mathrm{d}t$ is the time-derivative operator, can be derived passing in the Laplace domain and then using the bilinear transform for switching into the Z-domain [14]. Under the proper adaptation condition, $Z = 1/(2F_sC)$, where F_s is the sampling frequency, a power-normalized WD capacitor is implemented using a simple delay element z^{-1}. Analogously, an inductor, described by the equation $V = L\mathrm{d}I/\mathrm{d}t$, where L is the inductance, is adapted setting $Z = 2F_sL$ and its implementation turns out to be a delay element with the minus sign $-z^{-1}$.

D. Nonlinear Diode

If we describe a diode using the Shockley model the relationship between current I and voltage V is

$$I = I_s\left(e^{V/(\eta V_t)} - 1\right) \tag{7}$$

where e is Napier's number, V_t is the thermal voltage, η is the ideality factor and I_s is the saturation current of the diode. Using the approach based on the Lambert Function W [16], developed in the voltage WD domain firstly in [17], [18] and then extensively in [10], we derive the wave mapping

$$b = a - \frac{\eta V_t}{\sqrt{Z}} W\left(\frac{ZI_s}{\eta V_t} e^{\left(2a\sqrt{Z} + ZI_s\right)/(\eta V_t)}\right) + \sqrt{Z} I_s \ . \tag{8}$$

It is worth noticing that, using classical WDFs theory, a diode characterized by the nonlinear eq. (8) cannot be adapted.

E. Series and Parallel Adaptors

As well explained in [14], we can express a WD M-port series or parallel junction in matrix form as $\mathbf{b} = S\mathbf{a}$. $\mathbf{a} = [a_1, \ldots, a_M]^T$ and $\mathbf{b} = [b_1, \ldots, b_M]^T$ are the transposed vectors of the incident and reflected waves respectively (denoting the superscript T transposition), while S is an orthogonal scattering matrix, whose cells are functions of the corresponding port impedances, named $Z_1, \ldots, Z_M$.

In the case of a series junction, S can be written as

$$S = E_M - \sqrt{\alpha_s}\sqrt{\alpha_s}^T \ , \quad \alpha_s = \frac{2}{\sum_{j=1}^{M} Z_j}[Z_1, \ldots, Z_M]^T \ ,$$

where E_M is the $M \times M$ identity matrix. We can derive a series adaptor from the described series junction, making the i-th port reflection free, if we impose the adaptation condition $Z_i = \sum_{j=1, j\neq i}^{M} Z_j$.

Conversely, for a parallel junction we have

$$S = -E_M + \sqrt{\alpha_p}\sqrt{\alpha_p}^T \ , \quad \alpha_p = \frac{2}{\sum_{j=1}^{M} \frac{1}{Z_j}}\left[\frac{1}{Z_1}, \ldots, \frac{1}{Z_M}\right]^T \ .$$

Also in this case we can derive a parallel adaptor, making the the i-th port reflection free, if we set $Z_i = 1/\sum_{j=1, j\neq i}^{M} {Z_j}^{-1}$.

III. NL Bipole Dynamic Adaptation

In this section we describe a strategy for dynamically updating the port impedance of a NL instantaneous bipole in order to ensure adaptation at each time step. We discuss both the case in which the port voltage V is a NL function of the port current I and the case in which V is a NL function of I. Then we show that, since the port impedance changes in the middle of each iteration n, we need to properly weight the incident and the reflected wave signals of the NL bipole.

A. Port Impedance Update

Let us consider a generic active or resistive bipole characterized by an instantaneous NL function F_V which relates the port current I to the port voltage V, so that we can write $V = F_V(I)$. Let us assume the derivative of F_V w.r.t. I to be always strictly positive, i.e.

$$\frac{\mathrm{d}F_V(I)}{\mathrm{d}I} > 0 \quad \text{for each } I.$$

Then let us refer to an instantaneous actual value of I as I_0. It follows that I_0 is related to an unique port voltage value V_0, defined as $V_0 = F_V(I_0)$. We will refer to the point P_0 with coordinates (I_0, V_0) as the *operating point* on F_V. Let us notice that the defined operating point P_0 on the NL F_V curve is in common with the tangent straight line having equation

$$V_0 = q + \lambda I_0 \ , \tag{9}$$

with

$$\lambda = \frac{\mathrm{d}F_V(I_0)}{\mathrm{d}I} \quad , \quad q = V_0 - \lambda I_0 \ . \tag{10}$$

It is worth noticing that eq. (9) is in the same form of eq. (4). It follows that we can model the bipole characterized by the NL function F_V at the operating point P_0 with a voltage generator having $V_g = q$ and $R = \lambda$.

In the light of this we want to find a strategy for dynamically adapting a WD NL bipole, treating it as a time-variant WD real generator. In other words we need to find the actual operating point P_0 at each iteration n, in order to derive the proper parameters q_n and λ_n using (10), where the subscript n refers to the n-th iteration. Once we have derived q_n and λ_n, we have to set $V_{gn} = q_n$ and $Z_n = \lambda_n$, in order to ensure adaptation for the iteration $n+1$. As a matter of fact, at the beginning of each iteration n, we dispose only of two informations at the NL bipole port: the actual value of the incident wave a_n and the old value of the port impedance Z_{n-1}. For this reason we need a NL function $H_I(a, Z)$, such that

$$I_{0n} = H_I(a_n, Z_{n-1}) \ . \tag{11}$$

Found I_{0n}, we easily derive also V_{0n}, using $V_{0n} = F_V(I_{0n})$. Now we have all the needed variables for computing λ_n and q_n (10).

In some cases it is easier to express the NL bipole port current I as a NL function F_I of the port voltage V. Let us assume

$$\frac{\mathrm{d}F_I(V)}{\mathrm{d}V} > 0 \quad \text{for each } V.$$

It follows the coordinates of the operating point P_0 on F_I are related by the equation $I_0 = F_I(V_0)$. The operating point P_0 on the F_I curve is in common with the tangent straight line having equation

$$I_0 = q + \lambda V_0 \ , \tag{12}$$

with

$$\lambda = \frac{\mathrm{d}F_I(V_0)}{\mathrm{d}V} \quad , \quad q = I_0 - \lambda V_0 \ . \tag{13}$$

We notice that eq. (12) is in the same form of eq. (6). It follows that we can model the bipole characterized by the NL function F_I at the operating point P_0 with a current source having $I_g = q$ and $R = 1/\lambda$. As already pointed out in Subsection II-B, a current source may be implemented as a voltage generator if we properly set its parameters. In this case we would have $V_g = -q/\lambda$ and $R = 1/\lambda$. As happens dealing with current-dependent NL functions, at each iteration n, we need to compute the suitable parameters λ_n and q_n, in order to ensure adaptation for the iteration $n+1$, setting $Z_n = 1/\lambda_n$. For finding the actual operating point P_0, we need a NL function $H_V(a, Z)$, such that

$$V_{0n} = H_V(a_n, Z_{n-1}) \ . \tag{14}$$

Found V_{0n}, we easily derive also I_{0n}, using $I_{0n} = F_I(V_{0n})$, and the parameters λ_n and q_n through (13).

As an example of NL bipole characteristic, Fig. 2 shows a diode curve with a tangent straight line passing through a generic operating point P_0. The equations for applying dynamic adaptation to a diode will be described in Section IV.

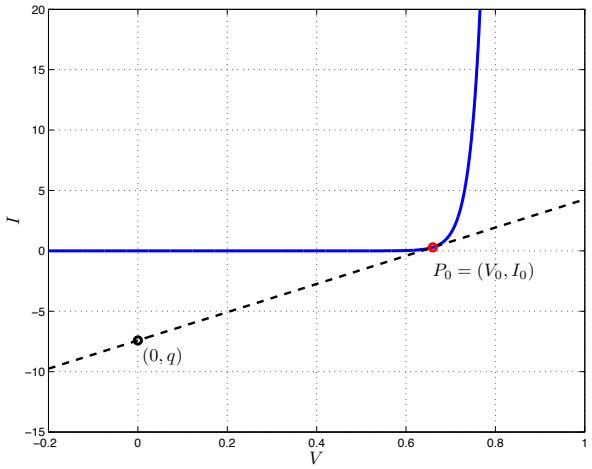

Fig. 2. Diode curve and its tangent line passing through the operating point $P_0 = (V_0, I_0)$ denoted by a red dot. The black dot has coordinates $V = 0$ and $I = q$. The slope of the black straight line is λ.

B. Wave Signals Weights Derivation

The NL bipole port impedance update, from Z_{n-1} to Z_n, described in Subsection III-A, occurs in the middle of each iteration, so it is out of phase w.r.t. the other variables updates taking place at the beginning or the end of the loop. It follows that, in the same iteration, some computations are performed using Z_{n-1} and some others using Z_n. This asynchrony characterizing the port impedance update prevent us considering our model as a classical time-varying power-normalized WD network [13], [14]. As a matter of fact, when the incident wave arrives at the NL bipole port, we change its port impedance. It follows that, in the n-th iteration, the port impedance Z_2 of the NL bipole is different w.r.t. the port impedance Z_1 of the adaptor to which the NL bipole is connected. At iteration $n+1$, Z_1 is updated with the old value of Z_2, while Z_2 changes again and so on. This discrepancy between Z_1 and Z_2 is not expected

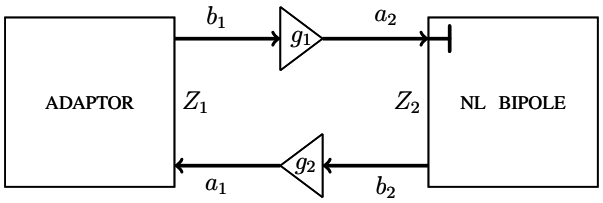

Fig. 3. Wave Weights in Dynamic Adaptation.

in classical power-normalized WDSs. In order to describe this phenomenon, let us call the port variables from the adaptor side with the subscript 1 (V_1, I_1, a_1 and b_1), while the port variables from the NL bipole side with the subscript 2 (V_2, I_2, a_2 and b_2). If Z_1 and Z_2 are different in the same iteration n, nobody assures us that the conditions

$$V_1 = V_2 \qquad I_1 = -I_2 \tag{15}$$

are true. In traditional time-varying power-normalized WDSs, conditions (15) are always automatically satisfied and this fact is highly desirable as V_1, V_2, I_1 and I_2 refer all to the same actual port. In order to cope with this problem, we introduce two weights g_1 and g_2, which filter the reflected waves b_1 and b_2, as shown in Fig. 3. According to Fig. 3 we can write $a_2 = g_1 b_1$ and $a_1 = g_2 b_2$. Let us assume for now to know a priori both Z_1 and Z_2 at iteration n. Applying the WD-K transformation (2), we can express the conditions (15) in the WD domain through the following system of equations

$$\begin{cases} (g_2 b_2 + b_1)\sqrt{Z_1} = (g_1 b_1 + b_2)\sqrt{Z_2} \\ (g_2 b_2 - b_1)\sqrt{Z_2} = (b_2 - g_1 b_1)\sqrt{Z_1} \end{cases} . \tag{16}$$

Solving the system (16) for g_1 and g_2, we obtain

$$g_1 = \frac{b_2\,(Z_1 - Z_2)}{b_1\,(Z_1 + Z_2)} + \frac{2\sqrt{Z_1}\sqrt{Z_2}}{Z_1 + Z_2} \quad , \tag{17}$$

$$g_2 = \frac{b_1\,(Z_2 - Z_1)}{b_2\,(Z_1 + Z_2)} + \frac{2\sqrt{Z_1}\sqrt{Z_2}}{Z_1 + Z_2} \quad . \tag{18}$$

We notice from (17) and (18) that if $Z_1 = Z_2$, $g_1 = g_2 = 1$ holds, as in traditional power-normalized WDSs. Therefore, in general, for ensuring conditions (15) to hold, it would be sufficient to set (17) and (18), avoiding to impose such constraints when $b_1 = 0$ or $b_2 = 0$. However, if we remove the assumption of knowing a priori both Z_1 and Z_2, according to what usually happens in practical applications, some problems arise. In fact, while satisfying the constraint (18) is easy, imposing the constraint (17) would require knowing the value of Z_2 before actually computing it. It follows g_1 can only be estimated and we will call such estimate $\hat{g}_1$.

Nevertheless, in practice, dealing with low frequency input signals and sufficiently high sampling frequencies F_s, the old value of g_1 turns out to be a good estimate $\hat{g}_1$. So in these cases $\hat{g}_1$ could be updated after Z_2 has been computed. Conversely, dealing with high frequency signals, the parameter λ might change so fast that the old value of Z_2 turns out to be too different from the right one. For this reason more advanced prediction techniques are under study.

IV. Diode Dynamic Adaptation

In this Section, as an example of application of the method described in Section III, we derive the equations needed for applying dynamic adaptation to a generic NL diode characterized by eq. (7). Eq. (7) expresses I as a function of V, so we search a NL function of the type (14). Therefore, using the Lambert function W [10] and exploiting hybrid relations among K and WD port variables easily derived combining (1) and (2), we obtain:

$$V = 2a\sqrt{Z} + ZI_s - \eta V_t\, W\left(\frac{ZI_s}{\eta V_t} e^{\left(2a\sqrt{Z} + ZI_s\right)/(\eta V_t)}\right) . \tag{19}$$

We need also the derivative of (7) w.r.t. V, which is

$$\frac{\mathrm{d}F_I(V)}{\mathrm{d}V} = \frac{I_s e^{V/(\eta V_t)}}{\eta V_t} \quad . \tag{20}$$

As $\mathrm{d}F_I(V)/\mathrm{d}V$ is dangerously near to zero at many operating points, we add it a small positive bias ϵ, in order to prevent numerical problems. Now we have all the information we need to find the coordinates of a generic operating point P_0 through (19) and (7). Consequently we are able to compute the parameters λ_n and q_n through (13) at each iteration n and to perform dynamic adaptation, setting $Z_n = 1/\lambda_n$.

V. Diode-based Audio Limiter

In this Section we propose an implementation of the audio limiter depicted in Fig. 4. As shown in Fig. 5 the corresponding WD network presents two nonlinearities (i.e. diodes) which are accommodated separately, preserving modularity as in linear WDSs. Diode D_1 is adapted "from the adaptor side" as in traditional WD networks, while diode D_2 is adapted using dynamic adaptation. As the two diodes are in antiparallel, we connected a two-port series adaptor to D_1 in order to ensure the orientations of D_1 and D_2 to be opposite.

The used implementation strategy is analogous to the one presented in [19], where a scanning of a treelike topological representation of the reference model (connection tree) is performed. In particular we have modeled the WDS in Fig. 5 as a Binary Connection Tree (BCT) [19], using series and parallel adaptors with up to 3 ports. The main difference w.r.t. the algorithm presented in [19] is that, thanks to dynamic adaptation, we can treat the NLE D_2 as a linear element (i.e. a leaf of the BCT). Conversely we accommodate D_1 as in classical NL WDF theory. Therefore D_1, characterized by the wave mapping (8), turns out to be the root of the BCT .

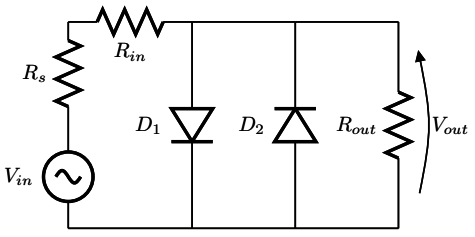

Fig. 4. Audio Limiter Reference Circuit.

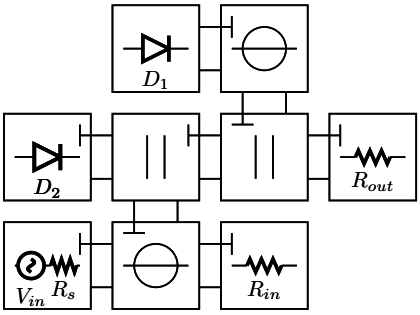

Fig. 5. Wave Digital Schema of the Audio Limiter in Fig. 4. Diode D_2 is adapted through Dynamic Adaptation.

As far as initial conditions are concerned, we assume all the initial port voltages and port currents to be zero. Therefore we initialize the port impedance of D_2 to $Z = \eta V_t / I_s$, as the starting operating point has coordinates $I_0 = 0$ and $V_0 = 0$. D_1 and D_2 are identical and the values of the Shockley model (7) parameters are: $\eta = 1$, $V_t = 0.025$ volts and $I_s = 10^{-12}$ amperes. The input signal V_{in} is provided by a real sinusoidal generator and it can be written as $V_{in}(n) = \rho \sin(2\pi f_0 n / F_s)$, where n indicates the n-th sample, ρ is the gain of the input signal, f_0 is its fundamental frequency and F_s is the sampling frequency. In the presented simulation we have $\rho = 1$ volt, $f_0 = 300$ Hz and $F_s = 48000$ Hz. The series resistance of the generator is $R_s = 1\ \Omega$, while $R_{in} = 3$ kΩ and $R_{out} = 50$ kΩ. The weight $\hat{g}_1$ is computed, after the update of the port impedance, as discussed in Subsection III-B. Moreover, as mentioned in Section IV, we add a small bias $\epsilon = 0.0005$ to the derivative estimate (20) in order to prevent numerical problems. Fig. 6 shows the trend of the output signal V_{out},

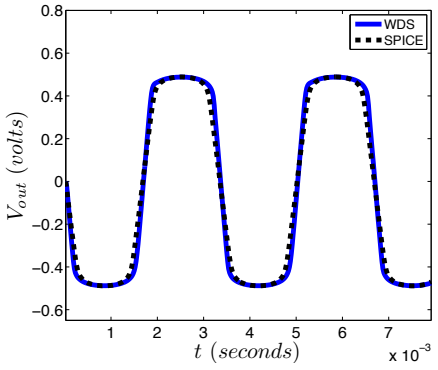

Fig. 6. V_{out} voltage detected across R_{out}. WD implementation versus SPICE result.

comparing the results of the WD implementation and SPICE. We notice that, even though the two results are quite similar, they do not coincide for two main reasons. The first reason is the weight estimation error $p = g_1 - \hat{g}_1$ and the second is the error due to the bias ϵ.

VI. Conclusion and Future Work

In this paper we have introduced the concept of dynamic adaptation of NL bipoles in WD networks. We have shown it is an effective method for accommodating multiple one-port NLEs in WDSs. The method works well with low-frequency input signals and reasonably high sampling frequencies, while it needs some improvements for high-frequency input signals. We are searching smarter prediction techniques in order to more effectively estimate the weight g_1.

We hope the presented results be the first step toward the formalization of new methods for adapting more complex nonlinearities.

References

[1] A. Fettweis, "Wave digital filters: Theory and practice," *Proc. of the IEEE*, vol. 74, pp. 270–327, Feb. 1986.

[2] G. De Sanctis and A. Sarti, "Virtual analog modeling in the wave-digital domain," *IEEE Trans. Audio, Speech, Language Process.*, vol. 18, pp. 715–727, May 2010.

[3] K. Meerkötter and R. Scholz, "Digital simulation of nonlinear circuits by wave digital filter principles," in *IEEE Int. Symp. Circuits Syst.*, vol. 1, June 1989, pp. 720–723.

[4] A. Sarti and G. De Poli, "Generalized adaptors with memory for nonlinear wave digital structures," in *Proc. European Signal Process. Conf. (EUSIPCO 1996)*, Trieste, Italy, Sept. 10–13 1996, pp. 1–4.

[5] ——, "Toward nonlinear wave digital filters," *IEEE Trans. Signal Process.*, vol. 47, pp. 1654–1668, June 1999.

[6] J. Pakarinen and M. Karjalainen, "Enhanced wave digital triode model for real-time tube amplifier emulation," *IEEE Trans. Audio, Speech, Language Process.*, vol. 18, pp. 738–746, May 2010.

[7] R. C. D. de Paiva, J. Pakarinen, V. Välimäki, and M. Tikander, "Real-time audio transformer emulation for virtual tube amplifiers," *EURASIP J. on Advances in Signal Process.*, Jan. 2011.

[8] A. Bernardini, K. J. Werner, A. Sarti, and J. O. Smith, "Modeling a class of multi-port nonlinearities in wave digital structures," in *Proc. European Signal Process. Conf. (EUSIPCO)*, Nice, France, Aug. 31 – Sept. 4 2015, pp. 669–673.

[9] ——, "Multi-port nonlinearities in wave digital structures," in *Proc. IEEE Int. Symp. Signals Circuits Syst. (ISSCS 2015)*, Iasi, Romania, July 9–10 2015.

[10] ——, "Modeling nonlinear wave digital elements using the lambert function," *accepted for publication in IEEE Trans. Circuits Syst. I, Reg. Papers*.

[11] K. J. Werner, V. Nangia, J. O. Smith, and J. S. Abel, "Resolving wave digital filters with multiple/multiport nonlinearities," in *Proc. 18th Conf. Digital Audio Effects (DAFx-15)*, Trondheim, Norway, Nov. 30 – Dec. 3 2015.

[12] T. Schwerdtfeger and A. Kummert, "Newton's method for modularity-preserving multidimensional wave digital filters," in *IEEE 9th Int. Workshop on Multidimensional (nD) Systems (nDS)*, Vila Real, Portugal, Sept. 7–9 2015, pp. 1–6.

[13] J. O. Smith, "Elimination of limit cycles and overflow oscillations in time-varying lattice and ladder digital filters," *Music Applications of Digital Waveguides*, vol. Technical Report STAN-M-39, CCRMA, Department of Music, Stanford University, p. 4778, 1987.

[14] S. Bilbao, *Wave and Scattering Methods for Numerical Simulation*, 1st ed., J. W. . Sons, Ed., New York, July 2004.

[15] K. Kurokawa, "Power waves and the scattering matrix," *IEEE Trans. Microwave Theory and Tech.*, vol. MTT–13, pp. 194–202, Mar. 1965.

[16] R. Corless, G. Gonnet, D. Hare, D. Jeffrey, and D. Knuth, "On the Lambert W function," *Advances in Computational Math.*, vol. 5, pp. 329–359, Dec. 1996.

[17] R. C. D. Paiva, S. D'Angelo, J. Pakarinen, and V. Välimäki, "Emulation of operational amplifiers and diodes in audio distortion circuits," *IEEE Trans. Circuits Syst. II, Exp. Briefs*, vol. 59, pp. 688–692, Oct. 2012.

[18] K. J. Werner, V. Nangia, A. Bernardini, J. O. Smith, and A. Sarti, "An improved and generalized diode clipper model for wave digital filters," in *Proc. 139th Conv. Audio Eng. Soc. (AES)*, New York, NY, Oct. 29 – Nov. 1 2015.

[19] A. Sarti and G. De Sanctis, "Systematic methods for the implementation of nonlinear wave-digital structures," *IEEE Trans. Circuits Syst. I, Reg. Papers*, vol. 56, pp. 460–472, Feb. 2009.